Numerical investigation of thermal stress and dislocation density in silicon ingot during a solidification process

Chen, Xuejiang
Research Institute for Applied Mechanics, Kyushu University

Nakano, Satoshi
Research Institute for Applied Mechanics, Kyushu University

Liu, Lijun
National Engineering Research Center for Fluid Machinery and Compressors, School of Energy and Power Engineering, Xi'an Jiaotong University, China | Research Institute for Applied Mechanics, Kyushu University

Kakimoto, Koichi
Research Institute for Applied Mechanics, Kyushu University

https://doi.org/10.15017/14183

出版情報：九州大学応用力学研究所所報. 135, pp.45-52, 2008-09. Research Institute for Applied Mechanics, Kyushu University
バージョン：
権利関係：

Numerical investigation of thermal stress and dislocation density in silicon ingot during a solidification process

Xuejiang CHEN*1, Satoshi NAKANO*1, Lijun LIU*1*2 and Koichi KAKIMOTO*1

E-mail of corresponding author: *xjchen@riam.kyushu-u.ac.jp*

(Received July 30, 2008)

Abstract

A transient global model was used to obtain the solution of a thermal field within the entire furnace during a unidirectional solidification process for photovoltaics. The melt-solid interface shape was obtained by a dynamic interface tracking method. The thermal stress distribution in the silicon ingot was solved using the displacement-based thermo-elastic stress model. Furthermore, the relaxation of stress and multiplication of dislocations were performed by using Haasen-Alexander-Sumino model (HAS model). The results revealed that levels of both residual stress and dislocation density are higher in the peripheral, bottom region than that in the internal region. The simulation results also suggested that the crucible constraint should be reduced for growing a silicon ingot with low thermal stress and low dislocation density.

Key words : *Computer simulation, multicrystalline silicon, Heat transfer, Solidification, Stresses, Dislocation*

1. Introduction

World solar photovoltaic (PV) market installations have been rapidly grown in recent years, reaching 2.8 GW in 2007 [1], and multicrystalline silicon is the most widely used material in solar cells. The unidirectional solidification method is cost-effective technique for large-scale production of multicrystalline silicon material for use in solar cells. There are two problems should be solved in unidirectional solidification process, improving the productivity of silicon, and improving the quality of silicon ingot, which means to reduce the impurities and defects/dislocations in the silicon ingot.

Since many dislocations and impurities in silicon materials limit their minority carrier lifetime, the dislocations and impurities in the silicon significantly affect the conversion efficiency of solar cells [2]. The simulation results from SINTEF [3] showed that the dislocation density in silicon ingot is directly related to the minority carrier lifetime. The experimental data from Arafune revealed that the minority carrier lifetime decreases as a function of dislocation density [2]. Therefore, reduction of the dislocation density, which is generated during growth from the melt of crystals, is needed to improve the quality of a silicon ingot.

Thermal stress is one of the major factors responsible for generation of dislocations during the solidification process. Because of nonuniform thermal deformation due to the temperature variation, thermal stresses are generated in a silicon ingot during solidification. When the effective stress exceeds the critical resolved shear stress (CRSS) of the material, dislocations are easily generated in the crystal.

With the development of modern computer technology, numerical simulation has been developed as a powerful tool for analysis and optimization of a crystal growth system. Many studies on optimization of a unidirectional process of crystalline silicon for solar cells have been carried out [4, 5, 6, 7, 8]. Liu calculated time-dependent distribution of iron and temperature [4], carbon concentration and SiC particle precipitation [5] in a silicon ingot. Two major types of casting furnaces, direct solidification system (DSS) and heat exchange method (HEM) system, have been compared from the aspects of thermal field, crystal quality and shear stress field by Wu [6]. A dislocation generation model was applied to the crystallization and subsequent cooling of silicon ingots in the experimental furnace at SINTEF [7]. A semi-analytical model was proposed to simulate thermal stress generation during experimental continu-

*1 Research Institute for Applied Mechanics, Kyushu University

*2 National Engineering Research Center for Fluid Machinery and Compressors, School of Energy and Power Engineering, Xi'an Jiaotong University, China

ous casting of polycrystalline silicon billets by Dour et al. [8], but they used one formulation of three parameters for calculating temperature. There have been few reports on numerical analysis of thermal stress and dislocations based on transient global heat transfer solution [9] in a unidirectional solidification process. Therefore, the main objective of this study was to establish numerical models of thermal stress and dislocation density in a silicon ingot based on transient global analysis, and use it to investigate the distribution of thermal stress and dislocation density in silicon ingot during a unidirectional solidification process. The relaxation of stress, dislocation multiplication and residual stress distribution were also analyzed.

2. Simulation model and method

To study the thermal field in the entire furnace for the unidirectional solidification process, an axisymmetric furnace shown schematically in Fig. 1 is simulated. The growth system consists of silicon melt, silicon ingot, crucible, pedestal, insulation shield and heater. The heat conduction, radiative exchange and melt flow are solved by the transient global model [4, 9], and the melt-solid interface shape is obtained by a dynamic interface tracking method.

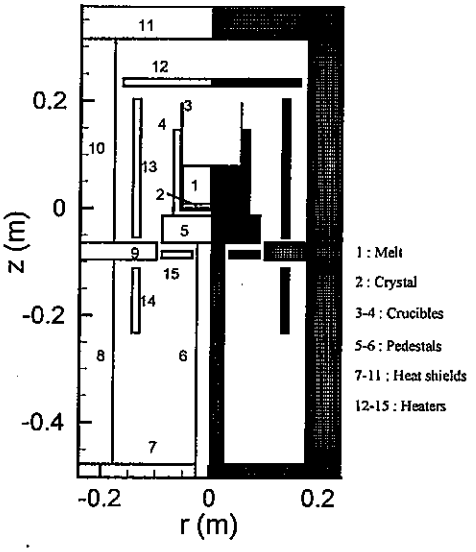

Fig. 1 Configuration, domain partition (left part) and computation grid (right part) of a unidirectional solidification furnace.

2.1 Modeling for thermal stresses

Since silicon has cubic crystal structure, and silicon is assumed to be solidified in a preferred direction ([001]), analysis of thermal stresses could be performed in the silicon ingot using an axisymmetric displacement-based thermo-elastic stress model, which was presented by Fainberg [10] for thermal stresses problems of anisotropic materials like semiconductor crystals. Since the gravity is negligible compared with the thermal stress, it is not considered in the equilibrium equations. The governing partial differential equations for momentum balance in an axisymmetric case can be written as

$$\frac{1}{r}\frac{\partial}{\partial r}(r\sigma_{rr}) + \frac{\partial}{\partial z}(\sigma_{rz}) - \frac{\sigma_{\varphi\varphi}}{r} = 0, \tag{1}$$

$$\frac{1}{r}\frac{\partial}{\partial r}(r\sigma_{rz}) + \frac{\partial}{\partial z}(\sigma_{zz}) = 0, \tag{2}$$

where σ_{rr}, σ_{zz} and $\sigma_{\varphi\varphi}$ are normal stresses in the radial, axial and azimuthal directions, respectively, and σ_{rz} is the shear stress.

For the Finite Volume Method (FVM), it is necessary to use an integral formulation in a control volume V of a solid material bounded by the surface S, which is transformed from Eqs. (1) and (2), written as

$$\int_S (\sigma_{rr}n_r + \sigma_{rz}n_z)dS - \int_V \frac{\sigma_{\varphi\varphi}}{r}dV = 0, \tag{3}$$

$$\int_S (\sigma_{rz}n_r + \sigma_{zz}n_z)dS = 0, \tag{4}$$

where n_r and n_z are the radial and axial components of the normal unit vector of surface S, respectively.

The stress-strain relation for an anisotropic thermoelastic solid body can be given by the following formulation:

$$\begin{pmatrix} \sigma_{rr} \\ \sigma_{\varphi\varphi} \\ \sigma_{zz} \\ \sigma_{rz} \end{pmatrix} = \begin{pmatrix} c_{11} & c_{12} & c_{13} & 0 \\ c_{12} & c_{22} & c_{23} & 0 \\ c_{13} & c_{23} & c_{33} & 0 \\ 0 & 0 & 0 & c_{44} \end{pmatrix} \begin{pmatrix} \varepsilon_{rr} - \beta_{11}\Delta T \\ \varepsilon_{\varphi\varphi} - \beta_{22}\Delta T \\ \varepsilon_{zz} - \beta_{33}\Delta T \\ \varepsilon_{rz} \end{pmatrix}, \tag{5}$$

where $\Delta T = T - T_{ref}$. In the above equation, β_{ij} is the thermal expansion coefficient and c_{ij} is the elastic coefficient of a silicon crystal. For cubic crystal lattices, there are only three independent coefficients c_{ij}, e.g., c_{11}, c_{12}, c_{44}. So for silicon, all other coefficients can be expressed in terms of those ones as follows, $c_{22} = c_{33} = c_{11} = 165.77\ GPa$, $c_{23} = c_{13} = c_{12} = 63.93\ GPa$, $c_{44} = 79.62\ GPa$. Also, $\beta_{11} = \beta_{22} = \beta_{33} = 4.5 \times 10^{-6}\ K^{-1}$. All properties of the silicon material are obtained from reference book [11]. The strains ε_{ij} can be calculated by

$$\varepsilon_{rr} = \frac{\partial u}{\partial r}, \quad \varepsilon_{\varphi\varphi} = \frac{u}{r},$$
$$\varepsilon_{zz} = \frac{\partial v}{\partial z}, \quad \varepsilon_{rz} = \frac{\partial u}{\partial z} + \frac{\partial v}{\partial r}, \tag{6}$$

where u and v are displacement components in the radial and axial directions, respectively. The final equations

for u and v displacements are obtained by substituting Eqs. (5) and (6) into Eqs. (3) and (4), and the two equations are solved iteratively by the FVM [10].

For the boundary conditions, the melt-solid interface is treated as no traction boundary, $\vec{\sigma}\cdot\vec{n}=0$, which means that the boundary can move freely. An axisymmetric boundary condition, $v=0, \partial u/\partial n=0$, is applied to the axial center. Since some coating materials, such as Si_3N_4, are used on crucible wall to reduce the crucible constraint for relaxing thermal stresses in silicon ingot, the boundary conditions at ingot/crucible wall interfaces are dependent upon crucible constraint. So two kinds of boundary conditions, without and with crucible constraint, are considered for the ingot/crucible wall interface. One is no traction boundary, $\vec{\sigma}\cdot\vec{n}=0$, which means that the effects of the crucible are ignored, and the other is rigid boundary, i.e., the displacements u and v on the interface are set to zero, which means the crucible constraint is considered strictly. As experiment shown, the real boundary conditions at ingot/crucible wall interfaces is between these two kinds of boundary conditions, and close to the rigid boundary condition.

After obtaining the distribution of u and v displacements, the stresses can be obtained from Eqs. (5) and (6). To represent the level of thermal stress components, the von Mises stress, σ_{von}, is introduced as

$$\sigma_{von}=\left(\frac{3}{2}S_{ij}S_{ij}\right)^{1/2}, \tag{7}$$

where S_{ij} is the stress deviator,

$$S_{ij}=\sigma_{ij}-\frac{1}{3}\sigma_{kk}\delta_{ij}. \tag{8}$$

2.2 HAS model for dislocation multiplication and stress relaxation

Time dependent creep deformation and dislocation multiplication are investigated in silicon ingot under high temperatures during a unidirectional solidification process. In present model, it is assumed that the silicon crystal is isotropic, neglecting crystal anisotropy. So the dislocation density analysis are carried out for only the [001] direction of a silicon crystal during the unidirectional solidification process.

In the dislocation model, the total strain could be sub-divided into elastic strain, thermal strain and creep strain, which could be given by

$$\varepsilon_{ij}=\varepsilon^e_{ij}+\varepsilon^T_{ij}+\varepsilon^c_{ij}, \tag{9}$$

where ε_{ij}, ε^e_{ij}, ε^T_{ij} and ε^c_{ij} are total strain, elastic strain, thermal strain and creep strain, respectively. The creep strain, ε^c_{ij}, is related to the dislocation density, which could be described by HAS model [12, 13]. In HAS model for multiaxial stress state [14], the creep strain rate, $\dot{\varepsilon}^c_{ij}$, and the multiplication rate of mobile dislocation density, $\dot{N}_m$, are given by

$$\dot{\varepsilon}^c_{ij}=\frac{1}{2}bk_0(\tau_{eff})^p\exp\left(-\frac{Q}{kT}\right)N_m\frac{1}{\sqrt{J_2}}\cdot S_{ij} \tag{10}$$

$$\dot{N}_m=Kk_0(\tau_{eff})^{p+\lambda}\exp\left(-\frac{Q}{kT}\right)N_m, \tag{11}$$

$$\tau_{eff}=\sqrt{J_2}-D\sqrt{N_m}, \tag{12}$$

$$J_2=\frac{1}{S_{ij}S_{ij}}, \tag{13}$$

where b is the magnitude of the Burgers vector, k is the Boltzman's constant, T is the absolute temperature in silicon crystal, Q is the Peierls potential, k_0, K, p and λ are some material constants, D is the strain hardening factor, S_{ij} and J_2 are the deviatoric stress and the second invariant of the deviatoric stress, respectively, and $\sqrt{J_2}$ indicates the equivalent shear stress. The expression of S_{ij} could be found in Eqn. (8). Especially for τ_{eff}, value of τ_{eff} is set equal to zero when $\sqrt{J_2}-D\sqrt{N_m}\le 0$, which means creep strain rate, $\dot{\varepsilon}^c_{ij}$, and multiplication rate of mobile dislocation density, $\dot{N}_m$, are always set equal to zero.

If the elastic strain in Eqn. (9) is applied to Hooke's law for an axisymmetric thermoelastic solid body, $\sigma_{ij}=c_{ij}\varepsilon^e_{ij}$, we can get the following formulation for stress relaxation:

$$\begin{pmatrix}\sigma_{rr}\\ \sigma_{\varphi\varphi}\\ \sigma_{zz}\\ \sigma_{rz}\end{pmatrix}=\begin{pmatrix}c_{11}&c_{12}&c_{13}&0\\ c_{12}&c_{22}&c_{23}&0\\ c_{13}&c_{23}&c_{33}&0\\ 0&0&0&c_{44}\end{pmatrix}\begin{pmatrix}\varepsilon_{rr}-\varepsilon^T_{rr}-\varepsilon^c_{rr}\\ \varepsilon_{\varphi\varphi}-\varepsilon^T_{\varphi\varphi}-\varepsilon^c_{\varphi\varphi}\\ \varepsilon_{zz}-\varepsilon^T_{zz}-\varepsilon^c_{zz}\\ \varepsilon_{rz}-\varepsilon^T_{rz}-\varepsilon^c_{rz}\end{pmatrix}. \tag{14}$$

When the creep strain rate and dislocation multiplication rate equations given by Eqs. (10) and (11) are solved with Eqn. (14) for stress relaxation by FVM iteratively, the dislocation multiplication analysis of silicon crystals, neglecting crystal anisotropy, can be performed.

3. Results and Discussion

3.1 Effects of crucible constraint on thermal stresses

The effects of crucible constraint on thermal stresses in a grown silicon ingot are discussed at first. The thermal stress is analyzed for two kinds of boundary conditions as described in section 2.. The von Mises stress

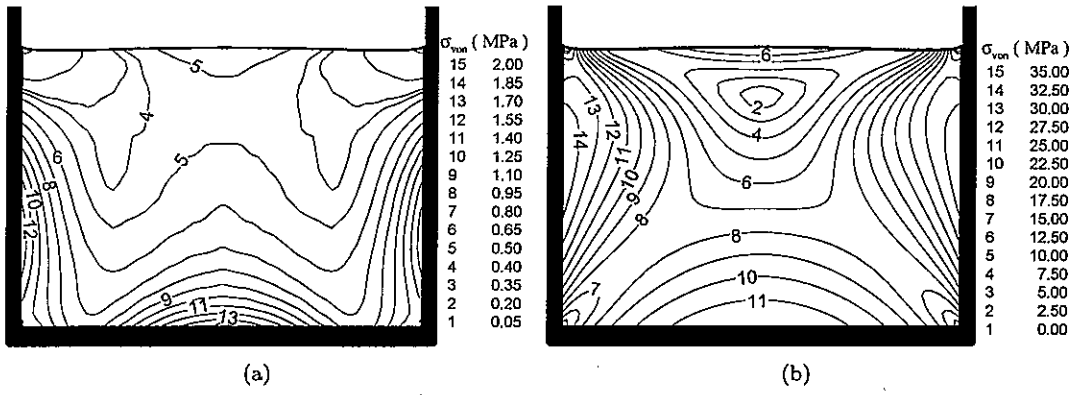

(a) (b)

Fig. 2 Von Mises stress distribution for (a) the no traction boundary condition, and (b) the rigid boundary condition on the ingot/crucible wall interface.

distribution in the silicon ingot, σ_{von}, is shown in Fig. 2. The results show that the stress distribution and its magnitude are completely different for the two different boundary conditions. In the case for the no traction boundary condition for ingot/crucible wall interface, the stresses are generated purely by the nonhomogeneous thermal field in the silicon ingot, and the ingot is subjected to the lower levels of stress than those in the case of a rigid boundary. The rigid boundary, on the other hand, produces a higher level of stress in the silicon ingot than that in the case of the no traction boundary. According to the excessive stress calculation equation,

$$\sigma_{ex} = \begin{cases} 0, & \sigma_{von} \leq \sigma_{crs} \\ \sigma_{von} - \sigma_{crs}, & \sigma_{von} > \sigma_{crs}, \end{cases} \qquad (15)$$

where σ_{crs} is the critical resolved shear stress, which is estimated to be $\sigma_{crs} = e^{(10.55+1.0147\times10^4/T)} \times 10^{-7}(MPa)$ for silicon [15]. The excessive stress in the whole ingot under the no traction boundary condition is zero, but that under the rigid boundary condition is calculated to range from 10 MPa to 35 MPa in most of the silicon ingot. Therefore, based on Jordan's theory [16], a silicon ingot grown under the rigid boundary condition is predicted to have more dislocations, but there would be no dislocations for the no traction boundary condition. A comparison with experimental data shows that the rigid boundary condition is close to the actual condition for the ingot/crucible wall interface, and this condition should therefore be applied for investigating the thermal stress distribution and dislocation density in a silicon ingot during the solidification process. From Fig. 2, it is clear that the boundary conditions on the ingot/crucible wall interface can change the thermal stress distribution, resulting in a different dislocation distribution in the silicon ingot. The results also suggest that it is important to use some coating materials, e.g. Si_3N_4, to reduce the crucible constraint in order to relax thermal stresses in silicon ingot during solidification process.

3.2 Thermal stresses for a solidification process

The time histories of heater power, fraction solidified and growth velocity of one solidification process are shown in Fig. 3. Variation of heater power as a function of time is set as a process parameter in this study. The heater power is decreased at a constant rate during the solidification process. Solidification is started at about 1 hour when the decrease of heater power is started. From time history of the solid fraction, we can see that the melt was solidified steadily through almost solidification process. The solidification time is close to 15 hours in this process. As the growth rate shown in Fig. 3, there are some oscillations in the growth rate at beginning because of the instabilities of melt flow. As solid fraction is less than 0.50, Rayleigh number of melt flow is larger than 1.0×10^5 [17], the convective flows in melt become unsteady (time-dependent). After that, as temperature difference in melt and height of melt are reduced, the melt flows become steady, then the growth rate goes to smooth.

The displacement vectors in the solidified ingot when the whole melt has been solidified are shown in Fig. 4. The displacement vectors clearly show how the ingot deforms. The magnitude of the deformation in the ingot is about 4 to 5 μm. The deformation is very small near the crucible wall because of the crucible constraint. The displacement vectors also reveal that the magnitude of deformation in the axial direction is much larger than that in the radial direction in most of the ingot, the reason being that the temperature gradient in the axial direction is larger than that in the radial direction. Fig. 5 shows temperature and von Mises stress distribution in silicon ingot during a solidification process at four different solid fractions, 0.40, 0.50, 0.75, 1.0, and

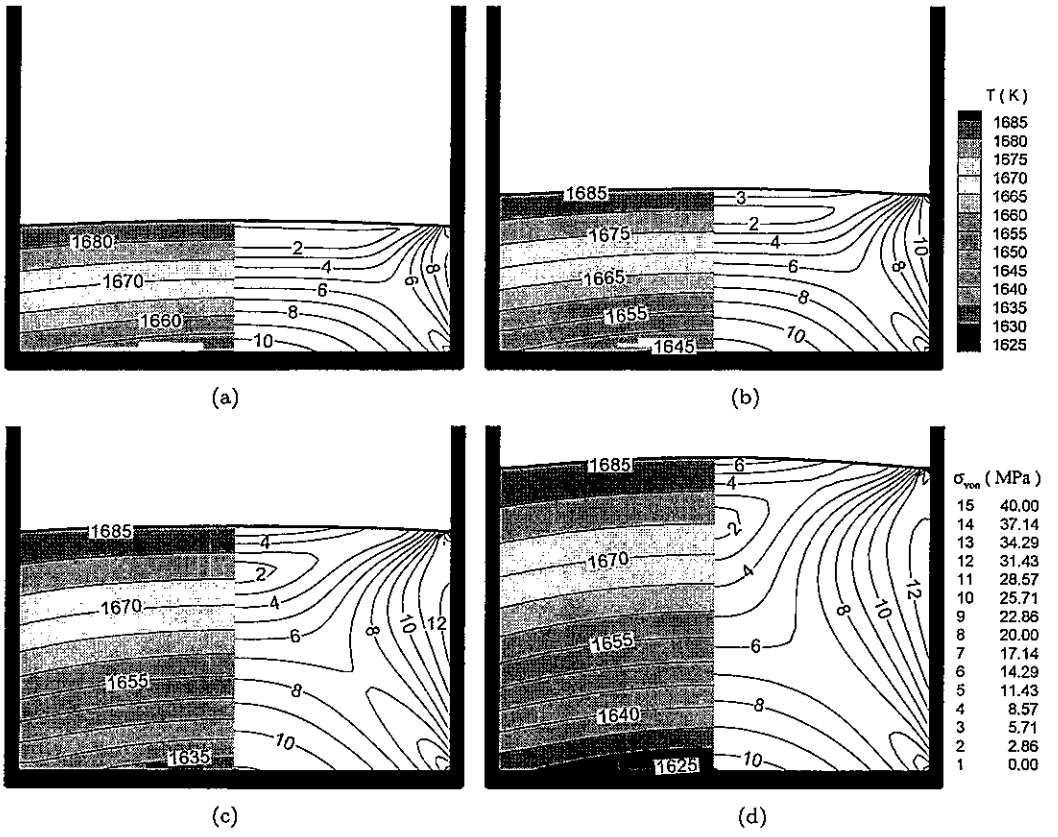

Fig. 5 Temperature (left part) and Von Mises stress (right part) distribution in the silicon ingot during a solidification process at different solid fractions: (a) 0.40, (b) 0.50, (c) 0.75, (d) 1.0.

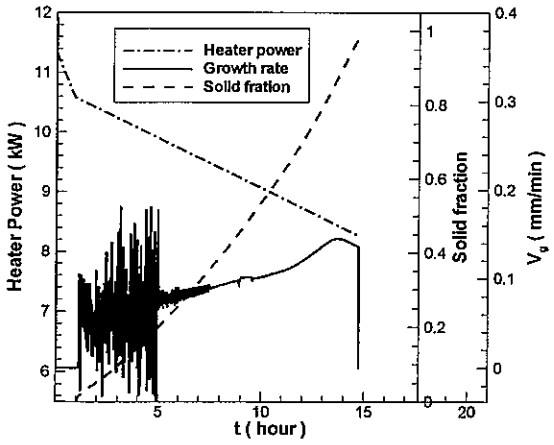

Fig. 3 Heater power, solid fraction and growth rate as a function of time during a solidification process.

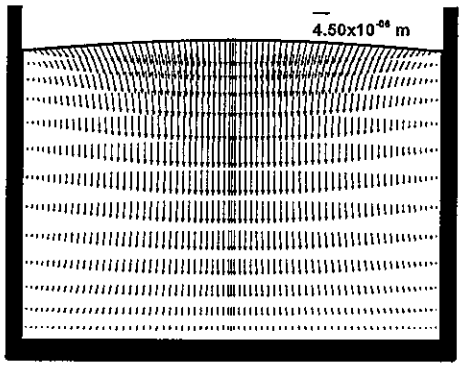

Fig. 4 Displacement vectors in the silicon ingot after a solidification process.

the time step is about 500 *mins*, 580 *mins*, 760 *mins*, 900 *mins*, respectively. Time solution reveals that thermal stresses are increased as the melt solidified because the temperature difference in ingot is increased as the melt solidified. It is also found from Fig. 5 that the stress levels are higher in the peripheral, bottom region than that in the internal region at each time step. The temperature distribution also reveals that the temperature gradient in solid is about 1 K/mm, which is lower than that of Czochralski crystal-growth system.

3.3 Effects of initial value of dislocation density

Since it is very difficult to make clear how many dislocations are introduced in a silicon ingot at each time step of the solidification process, it is necessary to impose the initial value of dislocation density in silicon ingot for investigation of stress relaxation and dislocation multiplication. From Eqs. (10) and (11), if initial value of dislocation density, N_{m0}, was strictly set equal to zero, $\dot{\varepsilon}^c_{ij}$, N_m and $\dot{N}_m$ would of course remain equal to zero, so the imposed initial dislocation density should be non-zero, and the sensitivity of the model to this value must be checked. To study the effects of initial value of dislocation density on the final results of dislocation density, and to find how many initial dislocations are reasonable for final dislocations, several non-zero values of N_{m0} (10^5 cm^{-2}, 10^4 cm^{-2}, 10^3 cm^{-2}, 10^2 cm^{-2}, 10^1 cm^{-2}) are uniformly imposed in silicon ingot to calculate the final dislocation density.

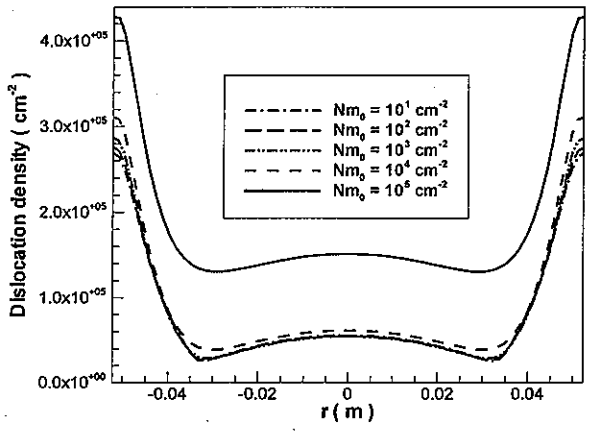

Fig. 6 Dislocation density distribution along radial direction at height of 66 *mm* from crucible bottom for several different initial dislocation densities after solidification process.

Fig. 6 shows dislocation density distribution along radial direction at height of 66 *mm* from crucible bottom for several different initial dislocation densities after solidification process. The figure shows that the final results of dislocation density are close to each other for small initial dislocation density, which means the effects of initial value on final results of dislocation density are very small. If the initial dislocation density is higher than 10^3 cm^{-2}, the final dislocation densities may be significantly different (dislocation density would be higher). As experimental data shown, the final dislocation density in silicon ingot is about $10^4 - 10^5$ cm^{-2}, so that we assume that the initial dislocation density is lower than 10^3 cm^{-2}.

3.4 Residual stress and dislocation density for a solidification process

One solidification process with 15 hours of solidification time is carried out to study the final results of residual stress and dislocation density in silicon ingot during solidification process. The time histories of this process can be found in Fig. 3.

Fig. 7 shows residual stress and dislocation density distribution in silicon ingot during a solidification process at four different solid fractions, 0.40, 0.50, 0.75, 1.0, and the time step is about 500 *mins*, 580 *mins*, 760 *mins*, 900 *mins*, respectively. The figures show that residual stresses in silicon ingot are increased as the melt solidified, especially near the edge part of silicon ingot. The reason could be found from Fig. 5 that the temperature difference and thermal stresses are increased as the melt solidified. For dislocation density in silicon ingot, as the melt solidified, the dislocation density in most of inner part of silicon ingot is not increased, while that is increased on the peripheral parts because of rapid increased thermal stresses. The contour shapes of residual and dislocation density are almost same, which indicates that thermal stresses are relaxed completely because of dislocation density, and also dislocations are multiplied completely because of thermal stress. It is also found from Fig. 7 that levels of both residual stress and dislocation density are higher in the peripheral, bottom region than that in the internal region after solidification process. This conforms to the results of thermal stress shown in Fig. 5, and also conforms to the simulation results obtained by the SINTEF group [7] showing that the dislocation density is maximum at the outer surface of a silicon ingot.

4. Conclusions

Numerical models of thermal stress and dislocation multiplication in silicon ingot for a unidirectional solidification process of multicrystalline silicon were established. Based on transient global heat transfer analysis, computations were carried out to investigate the distribution of thermal stress in a unidirectional solidification process of multicrystalline silicon for solar cells. The effects of crucible constraint were analyzed. The results suggested that it was important to reduce the crucible constraint in order to grow a silicon ingot with low thermal stresses and low dislocation density. Then, the relaxation of stress and multiplication of dislocations were performed by using HAS model. The results of effects of initial dislocation density showed that the effects on final results of dislocation density were very small for small initial values. Finally, the residual stress and dislocation density in silicon ingot for a solidification process

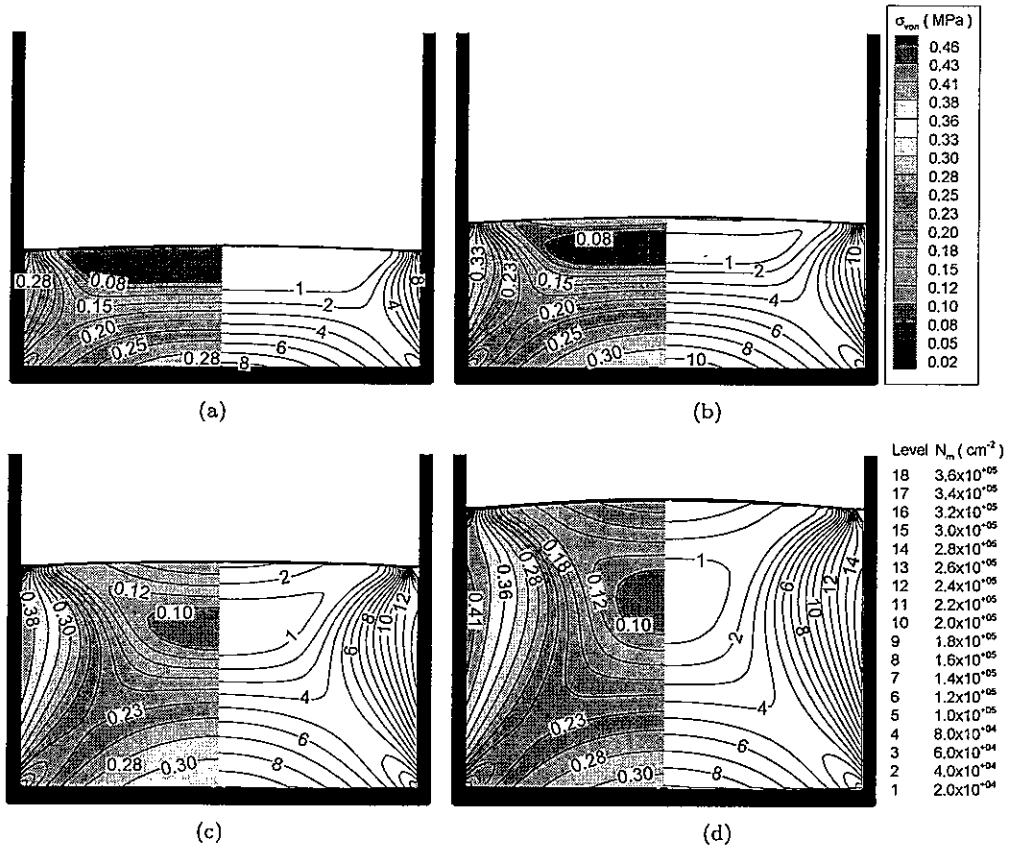

Fig. 7 Residual stress (left part) and dislocation density (right part) distribution in the silicon ingot during a solidification process at different solid fractions: (a) 0.40, (b) 0.50, (c) 0.75, (d) 1.0.

were also analyzed. The results revealed that levels of both residual stress and dislocation density are higher in the peripheral, bottom region than that in the internal region.

References

1) Marketbuzz™ 2008: Annual world solar photovoltaic industry report, (2008).

2) K. Arafune, T. Sasaki, F. Wakabayashi, Y. Terada, Y. Ohshita and M. Yamaguchi: Study on defects and impurities in cast-grown polycrystalline silicon substrates for solar cells, *Physica B*, Vol. 376-377, (2006) 236-239.

3) M. M'Hamdi, E. A. Meese, E. J. Øvrelid and H. Laux: Modelling of dislocation multiplication and associated minority carrier lifetime reduction during directional crystallization of silicon ingots, *Proceedings 20th European PVSEC*, (2005).

4) L. Liu, S. Nakano and K. Kakimoto: Dynamic simulation of temperature and iron distributions in a casting process for crystalline silicon solar cells with a global model, *J. Cryst. Growth*, Vol. 292, (2006) 515-518.

5) L. Liu, S. Nakano and K. Kakimoto: Carbon concentration and particle precipitation during directional solidification of multicrystalline silicon for solar cells, *J. Cryst. Growth*, Vol. 310, (2008) 2192-2197.

6) B. Wu, N. Stoddard, R. Ma and R. Clark: Bulk multicrystalline silicon growth for photovoltaic (PV) application, *J. Cryst. Growth*, Vol. 310, (2008) 2178-2184.

7) M. M'Hamdi, E. A. Meese, H. Laux and E. J. Øvrelid: Thermo-mechanical analysis of directional crystallisation of multi-crystalline silicon ingots, *Mater. Sci. Forum*, Vol. 508, (2006) 597-602.

8) G. Dour, F. Durand and Y. Brechet: Relaxation of thermal stresses by dislocation flow and multiplication in the continuous casting of silicon, *Modelling Simul. Mater. Sci. Eng.*, Vol. 5, (1997) 275-288.

9) L. Liu and K. Kakimoto: Partly three-dimensional global modeling of a silicon Czochralski furnace. I. Principles, formulation and implementation of the model, *Int. J. Heat Mass Transfer*, Vol. 48, (2005) 4481-4491.

10) J. Fainberg and H. J. Leister: Finite volume multigrid solver for thermo-elastic stress analysis in anisotropic materials, *Comput. Methods Appl. Mech. Eng.*, Vol. 137, (1996) 167-174.

11) W. Martienssen and H. Warlimont (Eds.): Handbook condensed matter and materials data, Springer, (2005).

12) H. Alexander and P. Haasen: Dislocation and plastic flow in the diamond structure, *Solid State Physics*, Vol. 22, (1968) 27-158.

13) M. Suezawa, K. Sumino and I. Yonenaga: Dislocation dynamics in the plastic deformation of silicon crystals II. thcoretical analysis of experimental results, *J. Appl. Phys.*, Vol. 51, (1979) 217-226.

14) N. Miyazaki: Dislocation density evaluation using dislocation kinetics model, *J. Cryst. Growth*, Vol. 303, (2007) 302-309.

15) N. Miyazaki, H. Uchida, T. Munakata, K. Fujioka and Y. Sugino: Thermal stress analysis of silicon bulk single crystal during Czochralski growth, *J. Cryst. Growth*, Vol. 125, (1992) 102-111.

16) A. S. Jordan, R. Caruso, A. R. VonNeida and J. W. Nielsen: A comparative study of thermal stress induced dislocation generation in pulled GaAs, InP, and Si crystals, *J. Appl. Phys.*, Vol. 52, (1981) 3331-3336.

17) D. Hurle(Ed.): Handbook of crystal growth, Vol. 2, Elsevier, (1994).